Phenylalanyl-tRNA Synthetase of *Escherichia coli* K 10. Multiple Enzyme·Aminoacyl-tRNA Complexes as a Consequence of Substrate Specificity†

Christine Güntner and Eggehard Holler*

ABSTRACT: The interaction between Phe-tRNA^{Phe} or other acyl-tRNA derivatives thereof and phenylalanyl-tRNA synthetase of *Escherichia coli* K 10 has been investigated by nonequilibrium dialysis, by fluorescence titration in the presence of 2-*p*-toluidinylnaphthalene-6-sulfonate, by the kinetics of the aminoacylation of tRNA^{Phe}, and by the kinetics of the catalytic hydrolysis of Phe-tRNA^{Phe}. Phe-tRNA^{Phe}, or derivatives thereof, forms two types of complexes with the synthetase. One type involves the attachment of the phenylalanyl moiety to the phenylalanine-specific site of the enzyme, and the other type, to the tRNA^{Phe}-specific binding site. They resemble alternative modes of a destabilized enzyme·product complex and are predicted on the basis of thermodynamic considerations. The two modes of binding of acyl-tRNA compete with each other. The attachment of Phe-tRNA^{Phe} to the phenylalanine-specific site dominates. At equilibrium, this complex is present at a fourfold higher concentration than the other type of complex. The HNO_2 deaminated Phe-tRNA^{Phe} binds exclusively to the site specific for L-phenylalanine. On the contrary, Ile-tRNA^{Phe} adds at 94.1% to the tRNA^{Phe}-specific site. The association of Phe-tRNA^{Phe} with this site leads to enzymatic hydrolysis into L-phenylalanine and tRNA^{Phe}. The complex involving the phenylalanine-specific site is hydrolytically unproductive. L-Phenylalanine acts as an activator of the hydrolysis by occupying the amino acid specific site and by shifting the equilibrium between the complexes toward the binding of Phe-tRNA^{Phe} at the tRNA^{Phe}-specific site. The association of Phe-tRNA^{Phe} at the phenylalanine-specific site does not interfere sterically with the binding of free tRNA^{Phe}. The sequential addition of free and aminoacylated tRNA^{Phe} exhibits negative cooperativity. Such a mechanism could help to expel the product from the enzyme.

Aminoacyl-tRNA synthetases are highly specific with respect to the esterification of a genetically related amino acid and tRNA. One of several mechanisms which accounts for the specificity (Holler, 1978) is the association of the synthetase with the correct amino acid and tRNA. The formation of complexes is selective because of the strong binding forces between a synthetase and the correct amino acid and tRNA, respectively. At first glance, this elegant way to accomplish specificity creates the problem that the fragments joined together in the aminoacyl-tRNA are predicted on the basis of free-energy calculations to give rise to an impractically high stability of the enzyme·product complex (Holler, 1978). If so, aminoacyl-tRNA synthetases could not be enzymatically active, because they would be blocked with the aminoacyl-tRNA. Not unexpectedly, measurements have revealed dissociation constants of the enzyme·aminoacyl-tRNA complexes that are far from those calculated and that are of the same magnitude as the dissociation constants for the substrate tRNAs (Holler, 1976; Jacques & Blanquet, 1977). Hence, the synthetases must have a device to destabilze the complexes with the aminoacyl-tRNA. In the present work we characterize two types of enzyme-phenylalanyl-tRNA complexes which are in the destabilized state.

Materials and Methods

Phenylalanyl-tRNA synthetase (EC 6.1.1.20) was prepared from *E. coli* K 10 in the presence of phenylmethanesulfonyl fluoride as described by Hanke et al. (1974). The specific activity was 53000 nmol mg^{-1} h^{-1}. Active sites (1.9) were titrated per mole of enzyme (Bartmann et al., 1975a). Phosphodiesterase (EC 3.1.4.1), inorganic pyrophosphatase (EC 3.6.1.1), alkaline phosphatase (EC 3.1.3.1), and pancreatic ribonuclease (EC 3.1.4.22) were purchased from Boehringer (Mannheim). Unfractionated tRNA was purified according to Zubay (1962) from *E. coli* K 10, tRNA^{Phe} [1] (acceptance 1540 pmol of L-phenylalanine per A_{260} unit) by methods including benzoylated DEAE-cellulose and reversed-phase chromatography (Egan & Kelmers, 1972). tRNA^{Phe} from *E. coli* MRE 600 (1200 pmol per A_{260} unit) was obtained from Boehringer (Mannheim). Uniformly labeled L-[^{14}C]phenylalanine (400–500 μCi/μmol) was purchased from Radiochemical Centre (Amersham), TNS and fluorescamine were from Serva (Heidelberg), L-β-phenyllactic acid and D,L-β-phenyllactic acid were from Sigma (St. Louis), and all other reagents of highest possible grade were from Merck (Darmstadt).

L-β-Phenyllactate Methyl Ester. The methyl ester was prepared by repeated incubation of 1 g of L-β-phenyllactic acid in 30 mL of dry methanol saturated with HCl for 2 days at room temperature. The product was twice recrystallized from ethyl acetate/petroleum ether at −20 °C. L-β-Phenyllactate methyl ester was obtained in 90% yield having a melting point (uncorrected) of 45 °C. The material was homogeneous as judged from thin-layer chromatography on silica gel (Estman Chromagram 13181 with fluorescent indicator 6060) using benzene as solvent. R_f values were 0.12 for the acid and 0.63 for the methyl ester (25 °C).

[^{14}C]Phe-tRNA^{Phe} was prepared as described (Bartmann et al., 1974) or with better yield by a modified procedure,

† From the Fachbereich Biologie und Vorklinikum, Universität Regensburg, D-8400 Regensburg, Federal Republic of Germany. *Received April 3, 1978; revised manuscript received January 18, 1979.* Dedicated to Professor Hermann Hartmann on the occasion of his 65th birthday.

[1] Abbreviations used: EDTA, (ethylenedinitrilo)tetraacetic acid; Tris, 2-amino-2-hydroxymethyl-1,3-propanediol; TNS, 2-*p*-toluidinylnaphthalene-6-sulfonate; Phe-tRNA^{Phe}, L-phenylalanyl ester of tRNA^{Phe}; Phe-tRNA$^{Phe}_{HNO_2}$, L-phenylalanyl ester of tRNA$^{Phe}_{HNO_2}$; Phe-tRNA$^{Phe}_{hv}$, L-phenylalanyl ester of tRNA$^{Phe}_{hv}$; Ile-tRNA^{Phe}, L-isoleucyl ester of tRNA^{Phe}; Phe(OH)-tRNA$^{Phe}_{HNO_2}$, DL-β-phenyllactyl ester of tRNA$^{Phe}_{HNO_2}$; L-Phe(OH)-tRNA$^{Phe}_{HNO_2}$, L-β-phenyllactyl ester of tRNA$^{Phe}_{HNO_2}$; tRNA$^{Phe}_{HNO_2}$, tRNA^{Phe} after treatment with nitrous acid; tRNA$^{Phe}_{hv}$, tRNA^{Phe} cross-linked between positions 8 and 13.

0006-2960/79/0418-2028$01.00/0

Table I: Nucleoside Composition of *Escherichia coli* tRNA^{Phe} and tRNA$^{Phe}_{HNO_2}$[a]

	U + T	G	A	C	I[f]	ψ	s^{4}U	m^{7}G	ms^{2}i^{6}A	fluorescence[b]
tRNA^{Phe}(native)[c]	7.6	23.2	14.6	20.1		2.8	1.0	1.0	1.1	1.0
tRNA$^{Phe}_{HNO_2}$[c]	8.2	23.4	13.5	20.8	1.2	2.7	1.1	1.0	1.0	0.05
Phe(OH)-tRNA$^{Phe}_{HNO_2}$[d]	8.4	23.2	13.4	19.9	0.8	3.1	1.0	1.0	0.9	0.05
tRNA^{Phe}(theor)[e]	8 + 1	23	14	21		3	1	1	1	1.0

[a] The results are given as the average of three determinations. [b] Relative fluorescence after reaction with fluorescamine. [c] Accepted 1540 pmol of phenylalanine per A_{260} unit. [d] 72% phenylalanylated. [e] Barrel & Sanger, 1969; Uziel & Khym, 1969. [f] Formed by HNO_2 treatment of tRNA^{Phe} or Phe-tRNA^{Phe}, respectively.

which involved phenol extraction, ethanol precipitation, desalting over a Sephadex G-25 fine column (0.7 × 50 cm), and again ethanol precipitation instead of the DEAE column.

DL-*β-Phenyllactyl-tRNA*$^{Phe}_{HNO_2}$. Twenty to fifty A_{260} units of Phe-tRNA^{Phe} in 0.5–3.5 mL of 0.1 M Tris-HCl buffer (pH 7.5) was mixed in an ice bath with 0.5 volume of a saturated solution of $NaNO_2$ (20 °C) and acidified with 0.005 volume of acetic acid. Deamination was allowed for 15 min at 25 °C. The mixture was returned to the ice bath, diluted with 0.1 volume of 20% (w/w) sodium acetate, and precipitated by the addition of 2.5 volumes of icy absolute alcohol. After 2 h at −20 °C, the precipitate was collected by centrifugation and redissolved in 3–10 mL of 0.1 M sodium acetate (pH 5), 0.2 M NaCl. The solution was applied to a small DEAE column (6 × 30 mm) mm) which had been equilibrated with the same buffer. After the column has been washed with 30 mL of buffer, the ionic strength was raised to 2 M NaCl whereby the acyl-tRNA was eluted during the first 3–6 fractions (15 drops/fraction). After precipitation with alcohol and drying under vacuum, the material was redissolved in 200 μL of 5 mM sodium acetate buffer (pH 5) and stored at −20 °C until it was used. tRNA$^{Phe}_{HNO_2}$ was obtained in the same way.

tRNA$^{Phe}_{HNO_2}$ was analyzed for its nucleoside composition in the following way: 1 A_{260} unit of modified tRNA was digested by incubating for 4 h at 45 °C in 50 μL of solution containing 0.2 M ammonium acetate (pH 8.5), 20 mM $MgCl_2$, 5 μg of snake venom phosphodiesterase, and 5 μg of alkaline phosphatase. For the determination of the 3′-end nucleoside, 1 A_{260} unit of modified tRNA was incubated in 50 μL of solution containing 0.1 M ammonium acetate (pH 7.5) and 5 μg of pancreatic ribonuclease during 2 h at 37 °C. The digested solutions were applied to a Beckman M 71 cation exchanger column (0.6 × 25 cm). Ammonium formate buffer (0.4 M) pH 4.15, was used as an eluant. A temperature of 50 °C, a pressure of 15 atm, and a flow rate of 0.45 mL/min were maintained. The UV absorption of the eluant was monitored simultaneously at 254 and 280 nm by a Spectra-Physics (Santa Clara, CA) dual-channel UV detector, Model 230, and recorded every 4 s with a Withof Transocomp 12-channel point recorder 288. For qualitative determination of the nucleosides, the elution volume of the nucleoside solution and the ratio of absorbance at 280 and 254 nm were compared with authentic standards.

Nucleotides and oligonucleotides are eluted in the breakthrough volume of the column (1.8 mL). Uridine, inosine, guanosine, adenosine, and cytidine elute at 3.6, 6.8, 9.1, 22.9, and 33.6 mL, respectively. Quantitative determination of nucleosides was performed by graphical integration of the appropriate peaks with an accuracy of ±2% per 0.05 A_{260} unit of analyzed nucleoside.

The base X (3′-*N*-(3′-amino-3-carboxypropyl)uridine) was identified by the reaction with fluorescamine (Sprinzl & Faulhammer, 1979). One A_{260} unit of tRNA in 100 μL of borate buffer (10 mM, pH 9.0) was treated under vigorous stirring at room temperature with five 5-μL portions of fluorescamine (100 mM in dry, spectroscopically pure acetone). After 15 min at room temperature, the mixture was diluted with 2.5 mL of 50 mM phosphate buffer (pH 7.0) and the fluorescence was determined using a Farrand MK-I spectrofluorometer. The spectra were taken at 25 °C at an excitation wavelength of 385 nm.

Table II: Binding of Native and HNO_2-Modified tRNA to Phenylalanyl-tRNA Synthetase and the Enzymatic Aminoacylation[a]

	binding	aminoacylation		amino acid acceptance (pmol/ A_{260} unit)
	K_{diss} (μM)	K_M (μM)	k_{cat} (s^{-1})	
tRNA^{Phe}	0.2[b]	0.20 ± 0.03	3.3 ± 0.3	1240 ± 20
tRNA$^{Phe}_{HNO_2}$	0.04 ± 0.01	0.17 ± 0.02	3.6 ± 0.3	1170 ± 30

[a] Binding of tRNA was followed via the synthetase-intrinsic fluorescence as described by Bartmann et al. (1975a). By this method, the association of the enzyme and a single molecule of tRNA is measured (Bartmann et al., 1975a). The dissociation constant, K_{diss}, for tRNA$^{Phe}_{HNO_2}$ was determined for the condition 0.02 μM enzyme, 0.005–1.0 μM tRNA$^{Phe}_{HNO_2}$, 0.05 M Tris-HCl buffer (pH 7.5), 10 mM $MgCl_2$, 0.1 mM EDTA, and 0.2 mM dithioerythritol at 25 °C. The symbols K_M and k_{cat} refer to the Michaelis–Menten and the catalytic rate constants, respectively. [b] Bartmann et al., 1975b.

As Table I indicates, HNO_2 treatment caused only minor modifications. One equivalent of adenosine was converted into inosine. The base X was deaminated in its 3-amino-3-carboxypropyl side chain. The degree of modification does not seem to depend on the prior phenylalanylation of the tRNA.

The completeness of the deamination of the phenylalanyl moiety was measured by thin-layer chromatography on poly(ethylenimine)–cellulose sheets (Polygram Cel 300 PEI/UV_{254} from Machery Nagel/Düren). Before chromatography, the [^{14}C]Phe(OH)-tRNA$^{Phe}_{HNO_2}$ (10 μCi/μmol of β-phenyllactate, 900 pmol per A_{260} unit) was stripped for 2 h at 37 °C in a solution containing 0.1 M sodium carbonate (pH 10.5). The solvent for the chromatography was 0.5 M potassium phosphate buffer (pH 5.8). The R_f values (25 °C) were 0.89 and 0.64 for L-phenylalanine and D,L-β-phenyllactate, respectively. More than 90% of the radioactivity migrated with the spot for D,L-β-phenyllactate. The remainder was associated with the spot for tRNA and was not changed despite a prolonged incubation at pH 10.5. Most probably, this material resembles a covalent side product of the HNO_2 treatment. Since our investigation did not indicate any interference that could be ascribed to this side product, the concentrations of Phe(OH)-tRNA$^{Phe}_{HNO_2}$ were corrected by assuming it unreactive.

In a series of control experiments, it was ascertained that tRNA$^{Phe}_{HNO_2}$ behaved like native tRNA^{Phe} (Table II). With

respect to hydrolysis into D,L-β-phenyllactate and $tRNA^{Phe}_{HNO_2}$, it is seen that Phe(OH)-$tRNA^{Phe}_{HNO_2}$ is approximately 50 times less sensitive than is Phe-$tRNA^{Phe}$ (Table III). This makes it a much easier compound with which to investigate the interaction between the synthetase and the acyl-tRNA.

[^{14}C]Phe-$tRNA^{Phe}_{HNO_2}$ was obtained by phenylalanylation of $tRNA^{Phe}_{HNO_2}$, which had been prepared by HNO_2 treatment of the native $tRNA^{Phe}$ (1200 pmol per A_{260} unit). The degree of charging was 1000 pmol of L-phenylalanine per A_{260} unit. Attempts to further increase the extent of aminoacylation of this preparation by repeated incubation with the aminoacylation mixture were unsuccessful.

[^{14}C]Phe-$tRNA^{Phe}_{hv}$ was prepared from $tRNA^{Phe}_{hv}$ by the method described for Phe-$tRNA^{Phe}$, however, in the presence of high concentrations of phenylalanyl-tRNA synthetase. In the case of 130 pmol of $tRNA^{Phe}_{hv}$, 100% were phenylalanylated in the presence of 30 pmol of enzyme and 50% in the presence of 5 pmol of enzyme. Preparative amounts (33 nmol of $tRNA^{Phe}_{hv}$, 8.1 nmol of enzyme) were 70% phenylalanylated with respect to 1200 pmol per A_{260} unit of the charging capacity of the originally native $tRNA^{Phe}$.

$tRNA^{Phe}_{hv}$ is obtained by UV-induced cross-linking of 4-thiouridine in position 8 with cytidine in position 13 (Favre & Yaniv, 1971). It was kindly donated by Dr. A. Favre (Paris). Quantitative determination by the borohydride method (Favre & Yaniv, 1971) indicated more than 99% of the $tRNA^{Phe}$ had been cross-linked. The kinetics of the association of enzyme and Phe-$tRNA^{Phe}_{hv}$ (not shown) are grossly different from those for Phe-$tRNA^{Phe}$ and do not indicate any second reaction at concentrations up to 8 μM Phe-$tRNA^{Phe}_{hv}$, suggesting that the amount of native $tRNA^{Phe}$ in the $tRNA^{Phe}_{hv}$ preparation is considerably less than 1%.

[^{14}C]Ile-$tRNA^{Phe}$ was prepared according to the method of Yarus (1972). Fifty A_{260} units of $tRNA^{Phe}$ was incubated with a reaction mixture resembling the one used for phenylalanylation except that 20% (v/v) methanol was present. The concentrations of isoleucyl-tRNA synthetase and L-[^{14}C]-isoleucine (10 μCi/μmol) were 1 μM and 0.4 mM, respectively, in a total volume of 4 mL. The reaction time was 15 min at 37 °C. $tRNA^{Phe}$ was isoleucylated at a level of 42%.

Hydrolysis of [^{14}C]Acyl-tRNA Catalyzed by Phenylalanyl-tRNA Synthetase. In a typical experiment, 250-μL reaction mixtures contained 0.1–2 μM [^{14}C]Phe-$tRNA^{Phe}$, 0.05–0.1 μM enzyme, 0.1 M Tris-HCl buffer (pH 7.5), 10 mM KCl, 10 mM $MgCl_2$, 0.1 mM EDTA, and 2 mM reduced glutathione. The mixture was preequilibrated for 2 min at 25 °C without the enzyme. Zero-time samples (50–100 μL) were drawn immediately before the addition of 20 μL of enzyme. Hydrolysis was followed by sampling 50–100 μL at time intervals. The samples were spotted on DEAE filter disks (Whatman DE 81), which had been presoaked and washed with 0.1 M glycine buffer (pH 2.3). The filters were then washed and counted as described (Santi & Anderson, 1974). In cases where the enzyme exceeded 1 μM, the samples were mixed with 50 μL of unfractionated tRNA (110 A_{260} units per mL, 0.25 M sodium acetate, pH 5) and precipitated with 10% trichloroacetic acid. The precipitates were collected and washed on GF/C filters as described (Kosakowski & Böck, 1970). The rate of hydrolysis was calculated in terms of the ratio of the initial rate of hydrolysis to the concentration of the enzyme. The values were corrected for spontaneous hydrolysis and plotted according to Eadie (1942) in Figure 5. The catalytic rate constant and the Michaelis–Menten constant were calculated from the intercept and the slope of the line, respectively. In single turnover experiments, the logarithm of the concentration of [^{14}C]Phe-$tRNA^{Phe}$ was plotted as a function of time. In all cases, the points were found to follow a linear relation (first-order kinetics), provided the concentration of the enzyme was at least five times the value of the dissociation constant of the enzyme·Phe-$tRNA^{Phe}$ complex. The catalytic rate constant was calculated from the slope of the line giving the best fit to the points.

Enzymatic Aminoacylation of tRNA. Conditions were basically those described by Kosakowski & Böck (1970). Precipitation of acyl-tRNA at low concentrations was achieved by including 5 A_{260} units of unfractionated tRNA in 0.5 M sodium acetate buffer (pH 5) immediately before the addition of 10% trichloroacetic acid. In some cases, [^{14}C]Phe-$tRNA^{Phe}$ was adsorbed on DEAE-cellulose filter disks (Santi & Anderson, 1974). The radioactivity was counted with an efficiency of 80% in the case of GF/C filters and of 63% in the case of DEAE filters. Preparations of nonradioactive Phe-(OH)-$tRNA^{Phe}_{HNO_2}$ were assayed for uncharged $tRNA^{Phe}_{HNO_2}$ using 100 μCi/μmol of L-[^{14}C]phenylalanine.

Nonequilibrium Dialysis. The method of Colowick & Womack (1969) has been previously used to measure the binding of amino acids to aminoacyl-tRNA synthetases (Kosakowski & Böck, 1971; Kosakowski & Holler, 1973; Hyafil et al., 1976). Here we used the method to determine the stoichiometry of enzyme·tRNA complexes. The principles underlying the method are discussed in the Appendix.

The dialysis system consisted of an upper chamber, which contained 0.8 mL of 0.05 M Tris-HCl (pH 7.5), 10 mM $MgCl_2$, 0.1 mM EDTA, 0.2 mM dithioerythritol, and a lower chamber of 1.4 mL containing the same buffer. Both chambers were stirred by magnetic bars. The upper chamber contained the enzyme and L-[^{14}C]phenylalanine, both at concentrations that were comparable with the value of the dissociation constant, 30 μM (Bartmann et al., 1975b), of the enzyme·L-phenylalanine complex. Dialysis occurred via a Visking dialysis membrane into the lower chamber. The exclusion limit was for particles with 10000–20000 molecular weight. The lower chamber was flushed with the buffer at a rate of 1.65 mL per min (LKB VarioPerpex pump with tubing having an inner diameter of 1 mm). The leaving buffer was collected in 1.2-mL fractions. The radioactivity of each fraction was spotted in 100 μL portions onto GF/C filter disks, which were dried and counted in 10 mL of toluene/0.5% 2,5-diphenyloxazole scintillation cocktail.

The titration was performed by adding 1-μL amounts of $tRNA^{Phe}$ or Phe(OH)-$tRNA^{Phe}_{HNO_2}$ to the upper chamber. Between each subsequent addition, three to four fractions were allowed to be collected. About this much time was needed to approach the steady-state rate of the appearance of the radioactivity in the effluent. At the end of the experiment, 20 μL of a concentrated solution of unlabeled L-phenylalanine was added to the upper chamber (final concentration of 2.5 mM). The collection of fractions was continued for several minutes.

The evaluation of the titration curve was accomplished by comparing the radioactivity (cpm) of the momentary steady-state concentration in the effluent with the radioactivity that would have been observed if all the L-[^{14}C]phenylalanine in the upper chamber were free to diffuse. Under the assumption that losses of radioactivity of the upper chamber during titration were negligible, the maximum radioactivity would correspond to that observed in the effluent after the addition of the unlabeled L-phenylalanine. The difference (Δcpm) between the momentary radioactivity and the

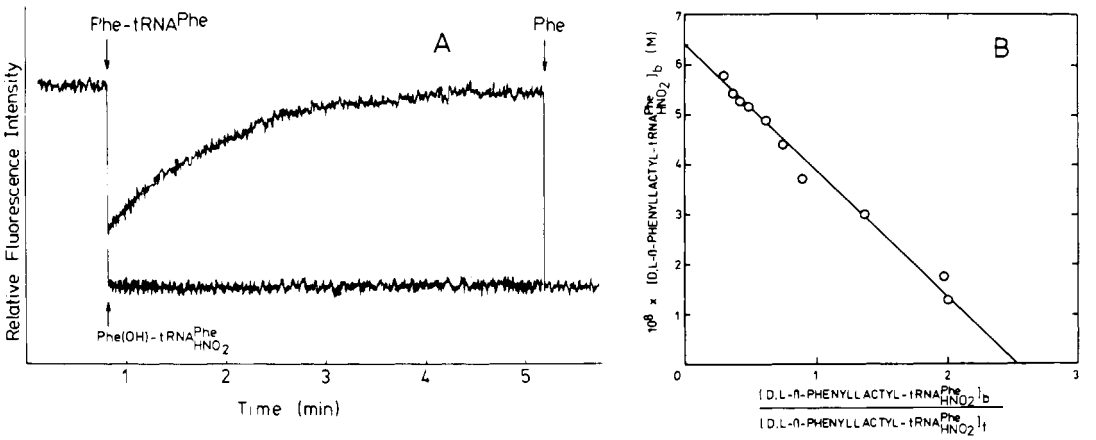

FIGURE 1: Displacement of TNS by the formation of the synthetase·acyl-tRNA complex is measured with a Hitachi Perkin-Elmer spectrofluorimeter. Conditions are 0.05 Tris-HCl (pH 7.5), 10 mM $MgCl_2$, 0.1 mM EDTA, 0.2 mM dithioerythritol, and 0.5 μM (A) or 0.06 μM (B) phenylalanyl-tRNA synthetase. (A) The fluorescence of the enzyme·TNS complex is recorded. At the time indicated, either 1.0 μM Phe-tRNA^{Phe} or 1.0 μM Phe(OH)-tRNA$^{Phe}_{HNO_2}$ is added; 5 mM L-phenylalanine is added at the end. This concentration causes the displacement of almost all TNS from the phenylalanine-specific binding site of the enzyme (Kosakowsi & Holler, 1973). (B) The degree of quenching of the fluorescence intensity in A is measured as a function of the concentration of Phe(OH)-tRNA$^{Phe}_{HNO_2}$. A plot according to Scatchard (1949) is obtained by the following method. The decrease of the fluorescence intensity (ΔF) is plotted as a function of the reciprocal concentration of the ligand. The points at the higher concentrations are fitted by a line. The line is extrapolated to infinite concentration and intersects the ΔF*axis* in ΔF_{Max}, the maximum degree of the fluorescence quenching when all binding sites of the enzyme are saturated with the ligand. The ratio of the amount of enzyme·ligand complex in relation to the total amount of the enzyme is $\Delta F/\Delta F_{Max}$ and the concentration of bound ligand is $\Delta F/\Delta F_{Max} \times [E]_0$ ($[E]_0$ is the analytical concentration of the enzyme). The concentration of free ligand (L_f) is calculated from the known concentration of the ligand added and from the concentration of the ligand bound (L_b). The calculated values are then plotted according to $[L]_b = [E]_0 - K_{diss}[L]_b/[L]_f$. The equation does not contain the number of binding sites since ΔF_{Max} has been obtained by the extrapolation to infinite concentration of the ligand. When the sites previously occupied by TNS add to the ligand uniformly, a straight line should be obtained, the slope of which can be used to calculate the dissociation constant, K_{diss}.

maximum radioactivity corresponds to the concentration of the enzyme·L-[^{14}C]phenylalanine complex. The difference is at maximum (Δcpm_0) when the titration has not yet begun. A titration curve is obtained by plotting the displaced radioactivity, $\Delta cpm_0 - \Delta cpm$, as a function of the added Phe(OH)-tRNA$^{Phe}_{HNO_2}$ or tRNA^{Phe}. The evaluation becomes complicated when the diffusion causes a considerable depletion of the radioactivity from the upper chamber as was the case in the present experiments. Instead of a single value for the maximum radioactivity, a time-dependent reference (curve R in the Appendix) had to be used. The differences Δcpm were then calculated at any point of the titration with reference to curve R. The curve is obtained by a graphical procedure explained in the Appendix.

Fluorescence Titration with 2-p-Toluidinylnaphthalene-6-sulfonate as Indicator. The weakly fluorescent dye 2-*p*-toluidinylnaphthalene-6-sulfonate has been shown to bind in a 1:1 ratio to the synthetase at the site specific for L-phenylalanine when concentrations of the indicator were below 10 μM (Kosakowski & Holler, 1973). At the same time it exhibits a strong increase of its fluorescence intensity. Binding of any ligand can be measured, which interacts with the phenylalanine-specific site and thereby displaces the indicator. Ligand association is observed as a decrease of the fluorescence intensity at 445 nm using an excitation wavelength of 366 nm. Measurements were performed at 25 °C with a Hitachi Perkin-Elmer fluorimeter Model MPF-2A as described (Kosakowski & Holler, 1973). The concentration of the indicator was usually 8 μM. Despite the competition between the dye and the added ligand, no corrections for the evaluation of dissociation constants were found to be necessary if low concentrations of the dye were applied (Kosakowski & Holler, 1973). Solutions were buffered with 0.05 M Tris-HCl (pH 7.5) and contained 0.1 mM EDTA, 0.2 mM dithioerythritol, and 10 mM $MgCl_2$.

Rapid Kinetic Measurements. Rapid kinetics were followed by observing the time-dependent fluorescence change after rapid mixing of the reactants in a Durrum-Gibson stopped-flow spectrophotometer equipped with a Durrum 16400 fluorescence attachment as has been described (Bartmann et al., 1975b). Buffer and 2-*p*-toluidinylnaphthalene-6-sulfonate had the same concentrations as for the equilibrium measurements. Exposure of Phe-tRNA^{Phe} to the buffer was reduced to a minimum period of time (usually less than 5 min) in order to minimize spontaneous hydrolysis.

Results

Synthetase·Acyl-tRNA Complexes Detected by Fluorescence Quenching. The mixing of phenylalanyl-tRNA synthetase with either Phe-tRNA^{Phe} or Phe(OH)-tRNA$^{Phe}_{HNO_2}$ in the presence of the fluorescent indicator TNS was followed by an immediate decrease of the fluorescence intensity (Figure 1A). In the case of Phe-tRNA^{Phe}, the decrease was succeeded by a slow recovery of the original fluorescence intensity. The effect depended on the presence of Mg^{2+}, as has been shown previously (Holler, 1976), and is close to maximum at 10 mM Mg^{2+}. In a control experiment using isoleucyl-tRNA synthetase instead of phenylalanyl-tRNA synthetase, it was verified that the fluorescence decrease did not occur with a noncognate synthetase (however, the fluorescence of the isoleucyl-tRNA synthetase·TNS complex is quenched upon the binding of the cognate substrates; Holler et al., 1971). Preparations of Phe-tRNA^{Phe}, which had been preincubated with 0.08 mg/mL of alkaline phosphatase (5 min at 25 °C in 0.1 M Tris-HCl buffer pH 7.5, 10 mM $MgCl_2$) to remove possible contaminations of AMP, gave comparable degrees of fluorescence quenching and subsequent slow recovery. Uncharged tRNA^{Phe} in the absence of Phe-tRNA^{Phe} or comparable concentrations of L-phenylalanine had no or negligible effects, respectively.

Other acyl-tRNAs were mixed with the synthetase using a stopped-flow spectrofluorimeter. The compounds were derived from Phe-tRNA^{Phe} carrying modifications in the acyl and the tRNA moiety (Table III). All acyl-tRNAs led to

Table III: Dissociation Constants of Synthetase·Acyl-tRNA Complexes Determined in the Presence of the Fluorescent Indicator 2-*p*-Toluidinylnaphthalene-6-sulfonate[a]

acyl-tRNA	$\Delta F_{Max}/\Delta F_{Phe\rightarrow\infty}$	K_{Diss} (μM)	hydrolysis rate constant × 10^{-3} s^{-1}
Phe-tRNA^{Phe}	0.75 ± 0.05	0.09 ± 0.01 0.1[b]	7 ± 2
Phe-tRNA$^{Phe}_{HNO_2}$	0.9 ± 0.1	0.017 ± 0.002	1.1 ± 0.1[c]
Phe(OH)-tRNA$^{Phe}_{HNO_2}$ DL-racemate	1.0 ± 0.1	0.03 ± 0.01[b]	0.13 ± 0.02[c]
Phe-tRNA$^{Phe}_{hv}$	0.13 ± 0.01	0.25 ± 0.03	≥8[c]
Ile-tRNA^{Phe}	0.059 ± 0.006	0.06 ± 0.02	1800 ± 200

[a] Reactants were mixed in a stopped-flow fluorimeter except where indicated. Reaction amplitudes were evaluated as described in the text. Maximum quenching of the fluorescence intensity is given with respect to the quenching in the presence of saturating amounts (5 mM) of L-phenylalanine. Rate constants are given for the synthetase-catalyzed hydrolysis of the acyl-tRNAs. Their measurements is described in the text. Conditions were 0.05 M Tris-HCl buffer (pH 7.5), 10 mM $MgCl_2$, 0.1 mM EDTA, and 0.2 mM dithioerythritol at 25 °C. [b] Fluorescence measured by the conventional spectrofluorimeter. [c] The liberation of [^{14}C]Phe was followed as described under Materials and Methods.

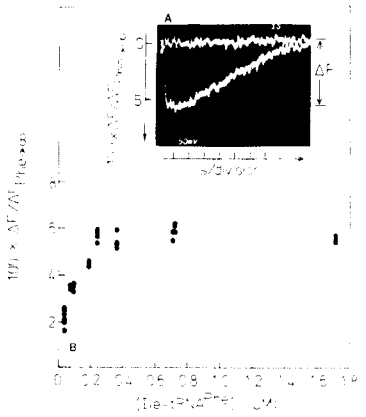

FIGURE 2: Displacement of TNS by Ile-tRNA^{Phe} measured with a stopped-flow fluorimeter. The emission of enzyme-bound TNS is followed using excitation light of 320 nm and a Corning 0-52 cut-off filter (75% transmittance at 370 nm) in the emission path as described (Bartmann et al., 1975b). Conditions are: 50 mM Tris-HCl buffer (pH 7.5), 10 mM $MgCl_2$, 0.1 mM EDTA, 0.5 mM dithioerythritol, 6 μM TNS, and 0.02–0.08 μM phenylalanyl-tRNA synthetase at 25 °C. (A) An oscilloscope tracing of the fluorescence intensity after mixing of 0.08 μM enzyme with 0.36 μM Ile-tRNA^{Phe}. The lower trace is followed by the upper trace. In the lower, the fluorescence intensity decreases rapidly followed by a slow recovery to the original intensity. The maximum decrease (ΔF) is used for the evaluation of the dissociation constant of the enzyme·Ile-tRNA^{Phe} complex. (B) ΔF is plotted as a function of the concentration of Ile-tRNA^{Phe}. Values of ΔF are given with respect to the decrease caused by saturating amounts of L-phenylalanine.

a decrease of the fluorescence intensity, the degree depending on the nature of the acyl and the tRNA moiety. The decrease was measured as a function of the concentration of the acyl-tRNA. In each case, the dependence was that of a saturation phenomenon indicating the formation of enzyme·acyl-tRNA complexes.

The saturation curves were evaluated for the dissociation constants of the complexes and for the decrease of the fluorescence intensity, ΔF_{Max}. The method of the evaluation is described under Figure 1. The plots according to Scatchard (Figure 1) were linear in all cases. The values of the parameters are summarized in Table III. The intensity decrease is given with respect to that measured for 5 mM L-phenylalanine under identical conditions. In the case of Ile-tRNA^{Phe}, where the degree of the aminoacylation of tRNA was only 41%, the possibility had to be considered that the uncharged tRNA^{Phe} could interfere with the formation of the enzyme·Ile-tRNA^{Phe} complex. The value for $\Delta F_{Max}/\Delta F_{Phe\rightarrow\infty}$ when the acyl-tRNA was in excess of the enzyme (Table III) was reexamined for the concentration of enzyme (0.32 μM) above the value of the dissociation constant (0.06 μM, Table III) and in excess of that for Ile-tRNA^{Phe} (0.18 μM). The intensity decrease was 2.9%. The concentration of the enzyme·Ile-tRNA^{Phe} complex is calculated to be 0.138 μM. If all enzyme could form the complex, the decrease (identical with $\Delta F_{Max}/\Delta F_{Phe\rightarrow\infty}$) should be 6.8%. This value is in agreement with 5.9% in Table III considering experimental accuracy. In the presence of excess enzyme, the uncharged tRNA^{Phe} is unlikely to inhibit the binding of Ile-tRNA^{Phe} due to the availability of free enzyme. The observed agreement suggests that in the range of the concentrations used in Figure 2 the interference by tRNA^{Phe} is negligible.

One of the facts seen in Table III is that the quenching of the fluorescence intensity responds to the structural variation in both the aminoacyl and the tRNA moiety. In the case of native tRNA^{Phe}, the noncognate isoleucyl moiety generates much less quenching of the fluorescence intensity than does the cognate phenylalanyl moiety. The introduction of the cross-link within the tRNA moiety is another reason for a reduction of the degree of quenching. The results suggest that, during the formation of the enzyme·acyl-tRNA, both the acyl and the tRNA moieties interact with specific subsites on the enzyme. The fact that the quenching of the fluorescence intensity can be interpreted in terms of a displacement of TNS from the phenylalanine-specific binding site (Kosakowski & Holler, 1973), together with the finding that the noncognate aminoacyl moiety has only a small effect, leads us to the working hypothesis that the acyl moiety of the enzyme-bond acyl-tRNA intrudes and interacts with the phenylalanyl-specific binding site (Holler, 1976).

The decrease of the fluorescence intensity after mixing of the synthetase and Phe-tRNA^{Phe} was followed by a slow recovery of the original fluorescence intensity. The same observation was made in the case of Ile-tRNA^{Phe} albeit the recovery was much faster (Figures 1 and 2 and Table III). The kinetics were first order in both cases under conditions where the enzyme was in excess over the acyl-tRNA and the concentrations were between five and ten times the values of the dissociation constants. The rate constants (0.007 and 1.8 s^{-1}, respectively) are in agreement with the kinetics measured by radioactive techniques, which follow the disappearance of acid-precipitable [^{14}C]Phe-tRNA^{Phe} (Figure 5; Yarus, 1972). The individual rate constants of the various acyl-tRNAs are given in Table III. There is a qualitative correlation between the ease of the catalytic hydrolysis and the inability of an acyl-tRNA to generate the fluorescence quenching.

Displacement experiments using uncharged tRNA^{Phe} were designed to see whether an acyl-tRNA binds to the enzyme via the tRNA^{Phe}-specific binding site. In one experiment (not shown), Phe-tRNA^{Phe} (1 μM) was added to a solution of 0.3 μM enzyme and varying concentrations of tRNA^{Phe} (0.5–10 μM) in the presence of 0.05 M Tris-HCl buffer (pH 7.5), 10 mM $MgCl_2$, 0.1 mM EDTA, 0.2 mM dithioerythritol, and 10 μM TNS at 25 °C. When the tRNA concentration increased from 0 to 3 μM, the fluorescence intensity dropped by approximately 50% of the decrease measured for the saturation of the enzyme by Phe-tRNA^{Phe}. From thereon, the intensity

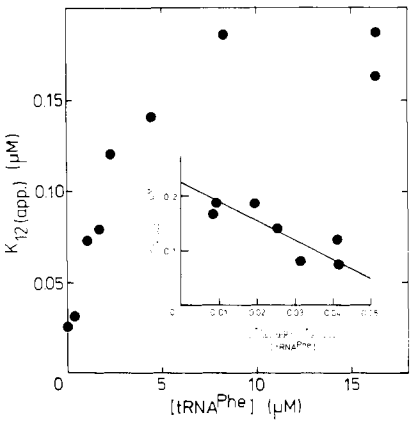

FIGURE 3: Effect of tRNA^{Phe} on the association of phenylalanyl-tRNA synthetase and Phe(OH)-tRNA$^{Phe}_{HNO_2}$. Titration experiments are carried out varying the concentration of Phe(OH)-tRNA$^{Phe}_{HNO_2}$ in the presence of tRNA^{Phe} at the concentrations indicated. Apparent dissociation constants for enzyme·acyl-tRNA complexes are determined as described under Figure 1. Their values are plotted in the inset according to eq 7. The line is supposed to give the best fit. Conditions are those of Figure 1 except for the enzyme (0.04 μM) and the tRNAs (0–17 μM tRNA^{Phe} and 0.004–8 μM Phe(OH)-tRNA$^{Phe}_{HNO_2}$).

was insensitive against further addition of tRNA^{Phe}. The results indicate the absence of competition and hence that the observed decrease of the fluorescence intensity is generated by the association of Phe-tRNA^{Phe} to a site other than that binding tRNA^{Phe}. The observed effect of tRNA^{Phe} demonstrates that the binding of the two ligands is coupled.

The anticooperative coupling for tRNA^{Phe} and an acyl-tRNA was investigated by measuring the dissociation constants for Phe-tRNA^{Phe} (stopped-flow method) and Phe(OH)-tRNA$^{Phe}_{HNO_2}$ (spectrofluorimeter) in the presence of varying concentrations of tRNA^{Phe} (Figure 3). The analysis is based on the reaction scheme shown in eq 1 for anticooperative binding. The various dissociation constants are defined by

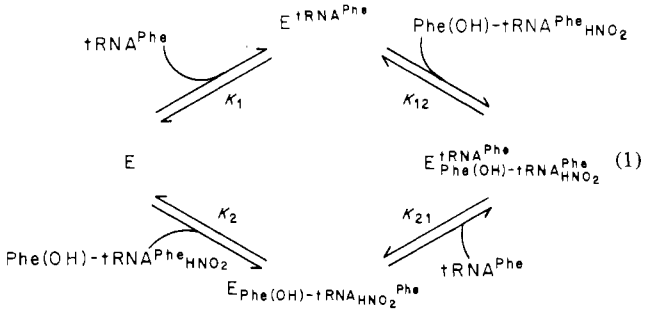

(1)

eq 2–5. At each concentration of tRNA^{Phe}, the concentration

$$K_1 = \frac{[E][tRNA^{Phe}]}{[E\cdot tRNA^{Phe}]} \quad (2)$$

$$K_2 = \frac{[E][\text{acyl-tRNA}]}{[E\cdot\text{acyl-tRNA}]} \quad (3)$$

$$K_{12} = \frac{[E\cdot tRNA^{Phe}][\text{acyl-tRNA}]}{[E\cdot tRNA^{Phe}\cdot\text{acyl-tRNA}]} \quad (4)$$

$$K_{21} = \frac{[E\cdot\text{acyl-tRNA}][tRNA^{Phe}]}{[E\cdot tRNA^{Phe}\cdot\text{acyl-tRNA}]} \quad (5)$$

of the acyl-tRNA was varied. The decrease of the fluorescence intensity was evaluated as described in the case of Figure 1. The dissociation constant is referred to as $K_{12(app)}$. This

Table IV: Dissociation Constants of Enzyme·tRNA^{Phe}·Acyl-tRNA Complexes[a]

	Phe-tRNA^{Phe}	Phe(OH)-tRNA$^{Phe}_{HNO_2}$ (racemate)
K_1 (μM)	0.4 0.2[c]	0.4
K_2[b] (μM)	0.09	0.026
K_{21} (μM)	8.5 ± 1.0[b]	3 ± 1[d]
K_{12} (μM)	1.9	0.21
K_{12}/K_2	21	8

[a] Fluorescence titrations with acyl-tRNAs were performed in the presence of various concentrations of tRNA^{Phe}. Apparent dissociation constants of the enzyme·acyl-tRNA complexes were determined as under Figure 1. They were used for plots as in Figure 3, inset, to determine the various dissociation constants in the table (see text). Conditions were similar to those under Figure 1 except for the concentrations of enzyme (0.04–0.1 μM) and tRNAs (0–17 μM tRNA^{Phe}, 0.004–8 μM Phe(OH)-tRNA$^{Phe}_{HNO_2}$, and 0.05–5 μM Phe-tRNA^{Phe}). [b] Taken from Table III, used to calculate K_{21} according to eq 7 (see text). [c] Obtained by titration with tRNA^{Phe} (Bartmann et al., 1975b). [d] Standard deviation for the slope of the plot (eq 7).

constant is related to the dissociation constants (eq 2–5) by eq 6, which has been derived for the synergistic binding of two ligands (Kosakowski & Holler, 1973). The equation can be

$$K_{12(app)} = K_2 \frac{K_{21}}{K_{21} + [tRNA^{Phe}]} \frac{K_1 + [tRNA^{Phe}]}{K_1} \quad (6)$$

rearranged into a form suitable for a linear plot of the experimental data (eq 7). Since the dissociation constant K_2

$$K_{12(app)} = \frac{K_2K_{21}}{K_1} - K_{21}\frac{K_{12(app)} - K_2}{[tRNA^{Phe}]} \quad (7)$$

for the enzyme·acyl-tRNA is known (Table III), the results $K_{12(app)}$ can be plotted against $(K_{12(app)} - K_2)/tRNA^{Phe}]$. The value of K_{21} is calculated from the slope of a linear fit of the experimental points (Figure 3, inset). The other constants can be calculated from the value of the intercept and from the relation $K_1K_{12} = K_2K_{21}$. The values of the dissociation constants, together with values of the coupling constants $K_{12}/K_2 = K_{21}/K_1$, are summarized in Table IV.

Synthetase·Acyl-tRNA Complexes Detected by the Displacement of L-[^{14}C]*Phenylalanine.* The dissociation of the enzyme·L-[^{14}C]phenylalanine complex was observed as a liberation of radioactivity when Phe(OH)-tRNA$^{Phe}_{HNO_2}$ was added. The concentration of the enzyme in the reaction mixture was far above the dissociation constant of the enzyme·acyl-tRNA complex and such that almost all added acyl-tRNA was incorporated into the complex. In a typical experiment, 23 μM enzyme and 23 μM L-[^{14}C]phenylalanine (522 μCi/μmol) were titrated by a stepwise addition of a total of 28 μM Phe(OH)-tRNA$^{Phe}_{HNO_2}$. From the 6900 cpm corresponding to the enzyme·phenylalanine complex in the absence of the acyl-tRNA, 4400 cpm was released. The released cpm and the concentration of the stepwise added ligand followed the expected linear relation. The extrapolation of the dependence to the point where all the enzyme·phenylalanine complexes would have been dissociated indicated a ratio of the concentrations of Phe(OH)-tRNA$^{Phe}_{HNO_2}$ to enzyme of 1.8. If the results of the fluorescence titration are assumed to indicate that the phenylalanine-specific binding site is no longer available when the enzyme is saturated with Phe(OH)-tRNA$^{Phe}_{HNO_2}$ (Table III), the value of 1.8 is interpreted as two molecules of Phe(OH)-tRNA$^{Phe}_{HNO_2}$ being required to achieve the saturation.

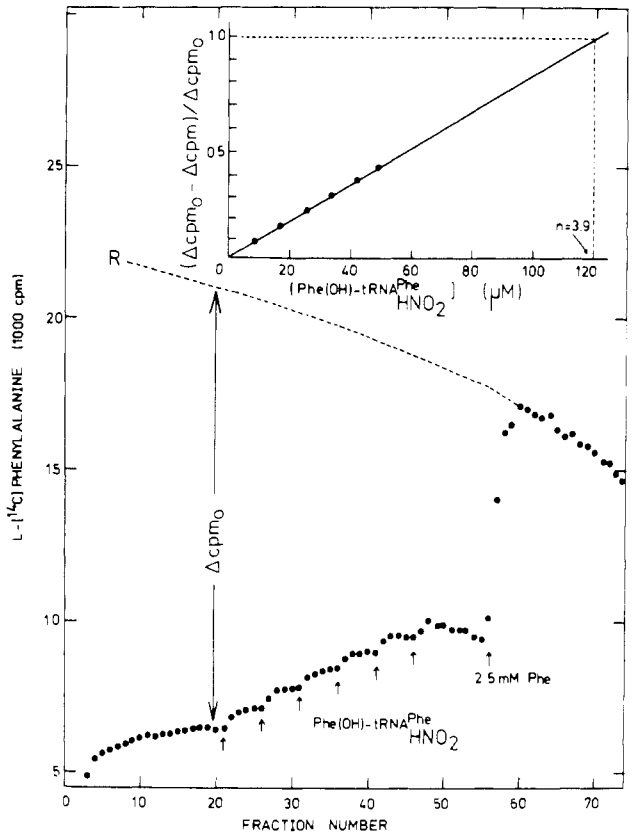

FIGURE 4: Dissociation of the enzyme·L-[^{14}C]phenylalanine complex during the titration with DL-β-phenyllactyl-tRNA$^{Phe}_{HNO_2}$. The increase of the dissociable L-[^{14}C]phenylalanine is observed by the non-equilibrium dialysis method. Conditions are: 0.05 M Tris-HCl buffer (pH 7.5), 10 mM $MgCl_2$, 0.1 mM EDTA, 0.2 mM dithioerythritol, 31 μM enzyme, 32 μM L-[^{14}C]phenylalanine (522 μCi/umol), and 155 μM tRNA^{Phe}. Portions of Phe(OH)-tRNA$^{Phe}_{HNO_2}$ are added as indicated by the arrows at concentrations given in the figure inset. The ordinate in the main figure refers to the radioactivity in the effluent fractions. The ordinate of the figure inset indicates the relative amounts of radioactivity that appears in the effluent due to the dissociation of the enzyme·L-[^{14}C]phenylalanine complex. The amounts are determined with the help of the reference curve as described under Materials and Methods and Appendix. The points in the inset are supposed to be part of a straight line, because the added Phe(OH)-tRNA$^{Phe}_{HNO_2}$ should be almost completely incorporated into the complex with the enzyme (see text). The point at $(\Delta cpm_0 - \Delta cpm)/\Delta cpm_0 = 1.0$ indicates the concentration of acyl-tRNA at which all of the enzyme·L-[^{14}C]phenylalanine complex is dissociated. An analogous method for the graphical evaluation of the stoichiometry of the ligand binding has been described (Bartmann et al., 1975a).

In another experiment, the reaction mixture contained in addition tRNA^{Phe}. The ratio of concentrations determined by the extrapolation was 3.9 (Figure 4). The concentration of tRNA^{Phe} was high enough to saturate both binding sites of the enzyme ($K_{diss(1)}$ = 0.08 μM and $K_{diss(2)}$ = 1.2 μM, Bartmann et al., 1975b). Despite the saturation, the displacement did occur strengthening the validity of the working hypothesis.

Phenylalanyl-tRNA synthetase is known to have two active sites (Bartmann et al., 1975a). The stoichiometry of approximately 4 molecules of Phe(OH)-tRNA$^{Phe}_{HNO_2}$ per molecule of enzyme has to be considered with respect to Phe(OH)-tRNA$^{Phe}_{HNO_2}$ as a racemate of D and L enantiomers. The inhibition constants for L-β-phenyllactate and D,L-β-phenyllactate in the aminoacylation assay were determined to be (3.7 ± 0.3) and (7.4 ± 0.5) mM, respectively, the inhibition being competitive against L-phenylalanine. The values differ by a factor of two. Such a discrepancy is expected if D-β-phenyllactate does not bind. A similar explanation could

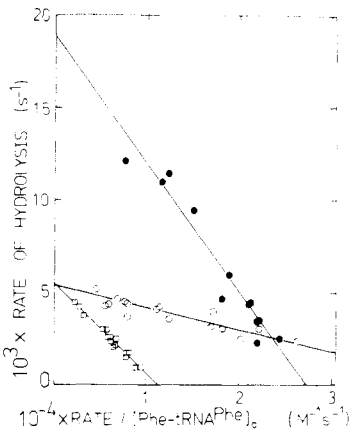

FIGURE 5: Hydrolysis of Phe-tRNA^{Phe} catalyzed by phenylalanyl-tRNA synthetase. Details of the experiment have been described under Materials and Methods. Initial rates are for Phe-tRNA^{Phe} alone (○), Phe-tRNA^{Phe} plus 1.0 μM tRNA^{Phe} (□), and Phe-tRNA^{Phe} plus 10 mM L-phenylalanine (●).

hold for the observed stoichiometry values of 2 and 4 in the case of Phe(OH)-tRNA$^{Phe}_{HNO_2}$ in the absence and the presence of tRNA^{Phe}, respectively. If D-β-phenyllactyl-tRNA^{Phe} does not bind, the true stoichiometries are 1 and 2 molecules of L-β-phenyllactyl-tRNA^{Phe}, respectively, binding to the phenylalanine-specific sites.

Enzyme·Acyl-tRNA Complexes Detected by the Inhibition of the Synthetase-Catalyzed Hydrolysis into Acid and tRNA. The hydrolysis of Phe-tRNA^{Phe} as catalyzed by phenylalanyl-tRNA synthetase is kinetically characterized by the Michaelis–Menten constant of 0.11 μM and the catalytic rate constant of 0.0054 s^{-1} (Figure 5, open circles). Free tRNA^{Phe} inhibits the hydrolysis competitively, the inhibition constant being 0.29 μM (Figure 5, open squares). The competitive inhibition and the magnitudes of the Michaelis–Menten constant and of the inhibition constant suggest that the enzymatic hydrolysis requires the association of Phe-tRNA^{Phe} at the tRNA-specific site of the enzyme.

The effect of L-phenylalanine at saturating concentrations (10 mM) was to increase the value of the catalytic rate constant by a factor of 3.5 and of the Michaelis–Menten constant by a factor of 6.4 (Figure 5). The results which were obtained at steady state have been verified at conditions of a single turnover of Phe-tRNA^{Phe} (14.6 μM enzyme, 8.6 μM Phe-tRNA^{Phe}, 0.05 M Tris-HCl buffer (pH 7.5), 10 mM $MgCl_2$, 0.1 mM EDTA, and 0.2 mM dithioerythritol). The rate constants were 0.0056 and 0.026 s^{-1} (a 4.6-fold difference) in the absence and presence of 4 mM L-phenylalanine, respectively. The effect of L-phenylalanine suggests that the sites on the enzyme binding the phenylalanyl moiety are not involved in the hydrolytic reaction. The activation effect is easily understood by an explanation considered in the Discussion.

Enzyme·Acyl-tRNA Complexes Detected by the Inhibition of the Enzyme-Catalyzed Aminoacylation of tRNA^{Phe}. According to Figure 6, Phe(OH)-tRNA$^{Phe}_{HNO_2}$ acts as a competitive inhibitor against L-phenylalanine. Using 8.3 ± 1.5 μM as the Michaelis–Menten constant for L-phenylalanine (filled circles), the inhibition constant was calculated from the slope of the line fitting the open circles to be 0.1 ± 0.04 μM. This value is in disagreement with the 0.03 μM for the dissociation constant of the enzyme·Phe(OH)-tRNA$^{Phe}_{HNO_2}$ complex because tRNA^{Phe} is present in the reaction mixture (4 μM) and because the binding of these tRNAs has been shown to be anticooperatively coupled (Table IV). The result is agreeable if compared with the value of $K_{12(app)}$ = 0.14 μM from Figure 3. In another experiment, the concentration of

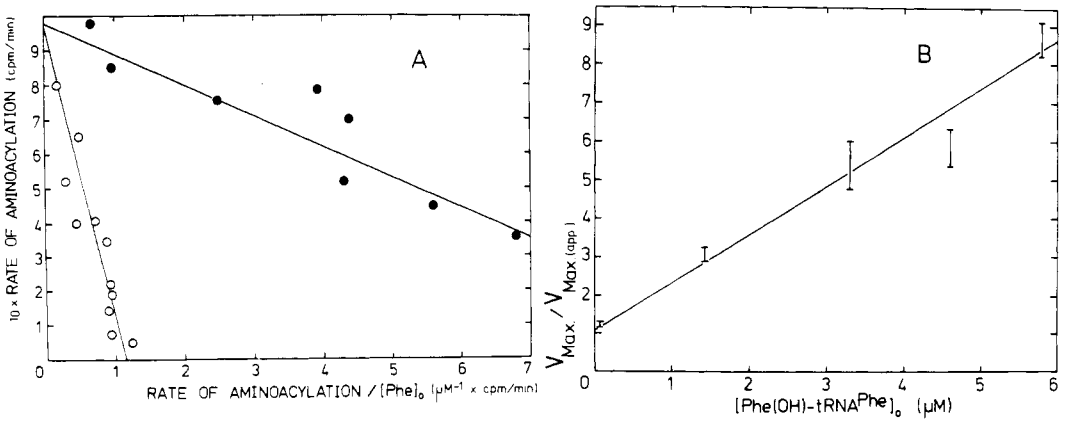

FIGURE 6: Phenylalanylation of tRNA^{Phe}. Inhibition by Phe(OH)-tRNA$^{Phe}_{HNO_2}$. (A) (○) Competition between L-[^{14}C]phenylalanine (4–440 μM, 10 μCi/μmol) and Phe(OH)-tRNA$^{Phe}_{HNO_2}$ (0.75 μM). (●) In the absence of the inhibitor. tRNA^{Phe} is 4 μM. (B) Secondary plot of $V_{Max}/V_{Max(app)}$ according to eq 9. The maximum rates are determined as described in the text. Aminoacylation is measured as a function of the concentration of tRNA^{Phe} (0.4–15 μM) at various fixed concentrations of Phe(OH)-tRNA$^{Phe}_{HNO_2}$ given in the figure. The concentration of L-[^{14}C]phenylalanine (100 μCi/μmol) is 0.25 mM. Conditions are otherwise: 0.1 Tris-HCl buffer (pH 7.5), 10 mM KCl, 10 mM $MgCl_2$, 2 mM reduced glutathione, 2 mM ATP, and 0.15–1.0 nM enzyme. Incubation time is 10 min at 28 °C.

tRNA^{Phe} was varied at various fixed concentrations of L-phenylalanine. Both the maximum rate and the Michaelis–Menten constant were affected. The value of the latter increased in accord with the anticooperative coupling when binding tRNA^{Phe} and Phe(OH)-tRNA$^{Phe}_{HNO_2}$. Furthermore, the increase leveled off at higher (>2 μM) Phe(OH)-tRNA$^{Phe}_{HNO_2}$ concentrations, indicating that the binding sites for the free and the acylated tRNA did not overlap.

The effect on the maximum rate was analyzed in detail. At the condition of the maximum rate, the concentration of tRNA^{Phe} is saturating. The observed variation as a function of the concentration of the inhibitor is thought to reflect the competition between L-phenylalanine and Phe(OH)-tRNA$^{Phe}_{HNO_2}$ to bind to the enzyme·tRNA^{Phe} complex. Equation 8 for competitive inhibition was assumed. $V_{Max(app)}$

$$V_{Max(app)} = V_{Max} \frac{[Phe]}{[Phe] + K_{M(Phe)}\left\{1 + \frac{[Phe(OH) - tRNA^{Phe}_{HNO2}]}{K_{12}}\right\}} \quad (8)$$

is the maximum rate determined from the Eadie plots (Eadie, 1942) at fixed concentrations of the inhibitor when the concentration of tRNA^{Phe} was varied. V_{Max} is the maximum rate in the absence of the inhibitor, $K_{M(Phe)}$ is the Michaelis–Menten constant of L-phenylalanine, and K_{12} is defined by eq 4. Equation 8 is rearranged to give eq 9. The values for

$$\frac{V_{Max}}{V_{Max(app)}} = 1 + \frac{K_{M(Phe)}}{K_{M(Phe)} + [Phe]} \frac{[Phe(OH)\text{-}tRNA^{Phe}_{HNO_2}]}{K_{12}} \quad (9)$$

$V_{Max}/V_{Max(app)}$ have been determined and are plotted in Figure 6 as a function of [Phe(OH)-tRNA$^{Phe}_{HNO_2}$]. It is seen that the data follow a linear dependence as is expected on the basis of eq 9. With the known values for $K_{M(Phe)}$ = 8.3 μM and [Phe] = 0.25 mM, the inhibition constant K_{12} is calculated from the slope of the line to be 0.2 μM. This value agrees with the result in Table IV. This agreement together with the observation of a linear dependence in Figure 6 reinforces the suggestions that (a) Phe(OH)-tRNA$^{Phe}_{HNO_2}$ binds (with the acyl moiety) to the phenylalanine-specific site of the enzyme, (b) the acyl-tRNA and tRNA^{Phe} may bind side by side, and (c) the binding of the acyl-tRNA of tRNA^{Phe} is anticooperative.

Discussion

Synthetase·Acyl-tRNA Complex Involving the Binding Site Specific for L-Phenylalanine. Acyl-tRNAs displace TNS or L-phenylalanine from the amino acid specific binding site of L-phenylalanyl-tRNA synthetase (Figures 1, 2, and 4; Table III). The extent varies as a function of the structure of the aminoacyl moiety. The competition between L-phenylalanine and Phe(OH)-tRNA$^{Phe}_{HNO_2}$ during the catalytic aminoacylation of tRNA^{Phe} is demonstrated in Figure 6. Both the displacement and the competition cannot be eliminated by the presence of saturating amounts of tRNA^{Phe}. The results are explained by assuming that the acyl-tRNA binds to the amino acid specific site of the enzyme. Moreover, they rule out mechanisms which employ an allosteric transition subsequent to the binding at the tRNA^{Phe}-specific site leading ultimately to the observed displacement of L-phenylalanine.

Synthetase·Acyl-tRNA Complex Involving the Binding Site Specific for tRNA^{Phe}. tRNA^{Phe} inhibits the enzymatic hydrolysis of Phe-tRNA^{Phe} competitively (Figure 5). The competition suggests that tRNA^{Phe} and Phe-tRNA^{Phe} bind to the same site on the enzyme. This site is productive for hydrolysis. A common binding site would be expected on the basis of the structural similarity of the free and the aminoacylated tRNA. However, a structural rearrangement of the tRNA appears to be invoked by its aminoacylation (Potts et al., 1977, and references therein).

The Binding of the Acyl-tRNA at the Phenylalanine-Specific Site Does Not Exclude the Association of tRNA^{Phe}. The addition of tRNA^{Phe} to a solution containing the synthetase·acyl-tRNA complex does not lead to the displacement of the acyl-tRNA (Table IV) nor does the presence of tRNA^{Phe} prevent the association of the enzyme and the acyl-tRNA (Figures 3, 4, and 6). It is concluded that tRNA^{Phe} and acyl-tRNA bind side by side to the enzyme at nonidentical sites.

The Different Modes of Complex Formation for the Acyl-tRNA Are Mutually Exclusive. Acyl-tRNAs may bind at either the phenylalanine-specific or at the tRNA^{Phe}-specific binding site of the enzyme. Provided the acyl-tRNA has free access to the amino acid specific binding site, increasing concentrations of the ligand should lead to a saturation of the enzyme. However, for most acyl-tRNAs, the fluorescent dye TNS could not be displaced from all of the enzyme despite the fact that the titration curves indicated the saturation with the ligand (Figure 2 and Table III). To account for the

observation, it is assumed that an acyl-tRNA cannot bind to the phenylalanine-specific site while another molecule of acyl-tRNA occupies the $tRNA^{Phe}$-specific site of the enzyme, and vice versa. As indicated by the magnitude of $\Delta F_{Max}/\Delta F_{Phe\rightarrow\infty}$, an acyl-tRNA with the proper side chain like that of Phe-$tRNA^{Phe}$ binds more frequently to the amino acid specific site than does an acyl-tRNA with an improper side chain, like that of Ile-$tRNA^{Phe}$ (Table III). If the rate constant of the enzymatic hydrolysis is taken as an indicator for the occupancy of the $tRNA^{Phe}$-specific site, it would seem that those acyl-tRNAs prefer the $tRNA^{Phe}$-specific site, which have a low tendency to add to the phenylalanine-specific site (small values for $\Delta F_{Max}/\Delta F_{Phe\rightarrow\infty}$ in Table III). The case is illustrated for Phe-$tRNA^{Phe}$ (Figure 7B). The value of $\Delta F_{Max}/\Delta F_{Phe\rightarrow\infty} = 0.75$ is interpreted as 75% of the complexes binding Phe-$tRNA^{Phe}$ at the phenylalanine-specific site and 25% carrying Phe-$tRNA^{Phe}$ at the $tRNA^{Phe}$-specific site. The catalytic rate constant for the enzymatic hydrolysis is 0.0054 s^{-1}. The amino acid binding site can be blocked by the addition of saturating amounts of L-phenylalanine. Since the $tRNA^{Phe}$-specific site of the enzyme should be still accessible to Phe-$tRNA^{Phe}$, all the enzyme ends up in carrying the acyl-tRNA at this binding site. In this complex, the enzyme is in the hydrolytically productive mode, explaining the observed 3.5–4.6-fold increase of the value of the catalytic rate constant for the hydrolysis (Figure 5). It should be emphasized that, although the hypothesis explains the observed activation of the enzymatic hydrolysis by L-phenylalanine (Figure 5), it does not account for the rapid hydrolysis of Ile-$tRNA^{Phe}$. Probably, an additional mechanism is functioning during the hydrolytic proofreading.

Structural Requirement for the Binding of an Acyl-tRNA to the Phenylalanine-Specific Site. The values of the maximum decrease of the fluorescence intensity, $\Delta F_{Max}/\Delta F_{Phe\rightarrow\infty}$, in Table III are thought to reflect in a first approximation the ability of an acyl-tRNA to bind to the phenylalanine-specific site. They indicate that (a) the α-amino group is not required, (b) the aminoacyl side chain is recognized, and (c) changes within the structure of the tRNA are important. (a) The nonessentiality of the amino group is reconcilable with the similarity observed between the values of the dissociation constants for the enzyme·L-phenylalanine methyl ester complex (0.75 mM, Kosakowski & Holler, 1973) and for the enzyme·L-β-phenyllactate methyl ester complex (3 mM, Güntner & Holler, unpublished), respectively. (b) The isoleucyl moiety has a value for $\Delta F_{Max}/\Delta F_{Phe\rightarrow\infty}$ which is smaller by a factor of 13 than that for the phenylalanyl moiety. The cognate aminoacyl moiety seems to be recognized by direct contacts with the amino acid binding site. (c) When compared with Phe-$tRNA^{Phe}$, the effect of a structural variation of the tRNA is found to be an increase of $\Delta F_{Max}/\Delta F_{Phe\rightarrow\infty}$ in the case of Phe-$tRNA^{Phe}_{HNO_2}$, and a decrease in the case of Phe-$tRNA^{Phe}_{hy}$. A comparison of the dissociation constants for the acyl-tRNAs and the corresponding acyl methyl esters above indicates that the interaction of the acyl moiety alone could not account for the observed binding affinities (Table III). A factor of 10^4 to 10^5 difference has to be explained by other interactions most probably involving parts of the transfer ribonucleic acid. Work is under way to elaborate the nature of the interaction.

Stoichiometry and the Coupling between the Sites Binding Phe-$tRNA^{Phe}$ and $tRNA^{Phe}$. Phenylalanyl-tRNA synthetase has been shown to consist of different subunits in a $(\alpha\beta)_2$-type structure (Fayat et al., 1974; Hanke et al., 1974). The synthetase has two active sites (Bartmann et al., 1975a) and associates with two molecules of L-phenylalanine and of $tRNA^{Phe}$. The association with each type of ligand follows negative cooperativity (Bartmann et al., 1975b). Saturation by $tRNA^{Phe}$ is followed by a loosening of the interaction between the synthetase and L-phenylalanine and by the elimination of the negative cooperativity for the amino acid (Bartmann et al., 1975b).

In the nonequilibrium dialysis experiment, one molecule of L-Phe(OH)-$tRNA^{Phe}_{HNO_2}$ is sufficient to displace the L-[^{14}C]phenylalanine from the complex. In the presence of saturating $tRNA^{Phe}$, two molecules are required (Figure 4). The finding is consistent with the observation of the negative cooperativity for L-phenylalanine and with the conclusion that the acyl-tRNA binds to the phenylalanine-specific site.

Anticooperative coupling (i.e., negative cooperativity) during the binding of unlike ligands is observed in the case of $tRNA^{Phe}$ and either Phe-$tRNA^{Phe}$ (Table IV) or Phe(OH)-$tRNA^{Phe}_{HNO_2}$ (Figure 3 and Table IV). Another example is the effect of $tRNA^{Phe}$ on the value of the inhibition constant for Phe-(OH)-$tRNA^{Phe}_{HNO_2}$ (Figure 6). Anticooperativity between the binding of L-phenylalanine and Phe-$tRNA^{Phe}$ accounts for the increase of the value of the Michaelis–Menten constant when the rate of the enzymatic hydrolysis was measured as a function of the concentration of Phe-$tRNA^{Phe}$ (Figure 5). Negative cooperativity has been reported for aminoacyl-tRNA synthetases specific for L-methionine (*E. coli*) (Blanquet et al., 1976), for L-tyrosine (*E. coli*) (Krauss et al., 1975; Mulvey & Fersht, 1977), for L-tyrosine (*Bacillus stearothermophilus*) (Fersht, 1975), for L-serine (yeast) (Krauss et al., 1975), for L-phenylalanine (yeast) (Fasiolo et al., 1977), for L-tryptophan (*E. coli*) (Muench, 1976), and for L-tryptophan (beef pancreas) (Zinoviev et al., 1977).

Do Other Aminoacyl-tRNA Synthetases Interact with Their Aminoacyl-tRNAs via the Amino Acid Recognition Site? Phe-$tRNA^{Phe}$ interacts with the phenylalanine binding site of the enzyme in competition with the interaction at the $tRNA^{Phe}$-specific binding site. The binding at the amino acid specific site dominates and can be measured. With other aminoacyl-tRNA synthetases the binding to the tRNA-specific site might dominate leaving the interaction with the amino acid specific site undetected. Isoleucyl-tRNA synthetase appears to be such a system since Ile-$tRNA^{Ile}$ could not displace L-[^{14}C]isoleucine (Königsbauer & Holler, unpublished). On the basis of kinetic mechanisms that have been published for methionyl-tRNA synthetase (*E. coli*) (Jacques & Blanquet, 1977) and arginyl-tRNA synthetase (Fersht et al., 1978), it is speculated that these systems exhibit the binding of the aminoacyl-tRNA to the amino acid specific sites.

Possible Function of the Novel Synthetase·Aminoacyl-tRNA Complex. As has been outlined during the introduction, the synthetases may use a mechanism which prevents a very tight binding of the aminoacyl-tRNA. The mechanism would be to destabilize the enzyme-aminoacyl-tRNA complex. The results presented here give information about the modes of binding assumed in the complex. In principle, three types of destabilized complex can be visualized (Figure 7A). (a) The aminoacyl-tRNA binds via the amino acid and the tRNA-specific sites. The complex is strained. (b) The aminoacyl-tRNA binds to the amino acid specific site. The complex is not strained. (c) The aminoacyl-tRNA binds to the tRNA-specific site. The complex is not strained. Our results are consistent with possibilities b and c. Case a seems to be ruled out by the competition experiments with L-phenylalanine or $tRNA^{Phe}$. The results show furthermore that a destabilization is inferred by the way of the anticooperative binding

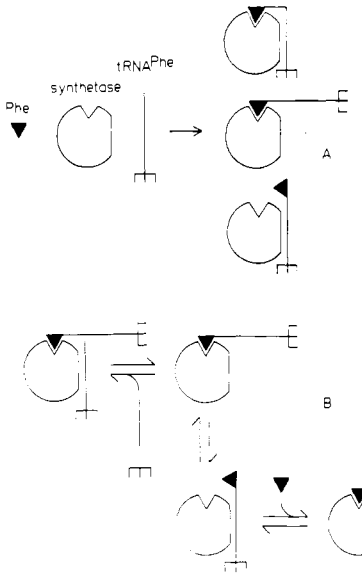

FIGURE 7: Schematic drawings of enzyme·Phe-tRNA^{Phe} complexes. Only a single active site is drawn because of simplicity. (A) Three modes of complexes; the upper case involves both the phenylalanine- and tRNA^{Phe}-specific sites, the middle only the phenylalanine-specific, and the lower only the tRNA^{Phe} specific site. (B) The reaction scheme of the displacement reactions. Addition of L-phenylalanine causes the displacement of Phe-tRNA^{Phe} from the phenylalanine-specific site. An increased rate of the enzymatic hydrolysis of Phe-tRNA^{Phe} is observed (Figure 5). Addition of tRNA^{Phe} causes the displacement from the tRNA^{Phe}-specific site without preventing binding to the phenylalanine-specific site (Figure 3; Table IV).

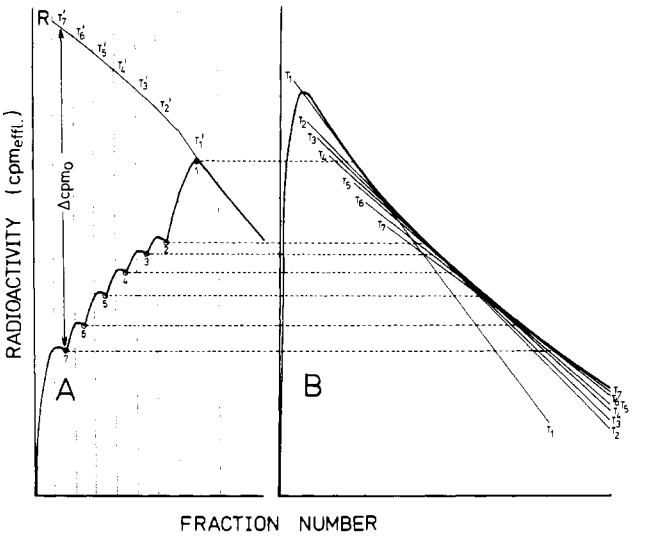

FIGURE 8: Radioactivity measured in the effluent during nonequilibrium dialysis. The dialysis chamber *not* containing the enzyme and the radioactive ligand (here [^{14}C]phenylalanine) is flushed by buffer as described in Materials and Methods. The radioactivity appearing after diffusion through the membrane is given in the figure as a function of the fraction effluent. (A) In the presence of enzyme, increasing amounts of a ligand are added at points 7 → 1. The ligand competes with [^{14}C]phenylalanine for binding to the enzyme. (B) In the absence of enzyme, the radioactivity in the effluent decreases exponentially. The rate of the decrease at a given radioactivity 1,..., 7 corresponds to the slope of the tangent T_1,..., T_7.

of uncharged tRNA^{Phe}. It remains to be investigated which are the elementary steps of the destabilizing reactions.

Appendix

Nonequilibrium Dialysis. Consider a dialysis system containing L-[^{14}C]phenylalanine in the upper chamber. Radioactivity diffuses across the membrane into the lower chamber and is eluted from there at a constant flow rate and is fractionated in samples of constant sizes. The rate of diffusion is proportional to the concentration of L-[^{14}C]-phenylalanine in the upper chamber that is free to diffuse

$$-d[Phe]/dt = f[Phe] \quad (10)$$

where $-d[Phe]/dt$ corresponds to the rate of decrease of the concentration in the upper chamber, [Phe] to the actual concentration, and f to a system specific diffusion constant. At steady state, each fraction of the effluent contains radioactivity in proportion to the concentration in the upper chamber (Colowick & Womack, 1969)

$$[Phe]_{effl} = F[Phe] \quad (11)$$

where $[Phe]_{effl}$ and [Phe] refer to the concentration of L-[^{14}C]phenylalanine in the effluent sample and in the upper chamber, respectively, and F to a second, system-specific constant. As a consequence of diffusion (eq 10), the concentrations of L-[^{14}C]phenylalanine in the upper chamber and in the effluent sample decrease exponentially with time. An example is given in Figure 8B. An important note is that each point of the curve belongs to a concentration of diffusible L-[^{14}C]phenylalanine in the upper chamber and the slope of the tangent corresponds to the instantaneous rate of decrease of this concentration (eq 10). Whatever the course of a titration curve (like curve A in Figure 8) will be, the rate of decrease and the momentary concentration are correlated by a curve such as that in Figure 8B in the absence of the enzyme.

Consider the upper chamber contains also the synthetase. Depending on the concentrations of enzyme and L-[^{14}C]-phenylalanine, part of the radioactivity will be bound in the form of the enzyme·L-[^{14}C]phenylalanine complex that cannot pass the membrane. This leads to a decrease of both the radioactivity in the effluent and its depletion from the upper chamber. During titration, the added ligand binds to either the same site as does L-[^{14}C]phenylalanine or to a second site. In the first case, it is the competition that evokes a displacement of radioactivity from the complex in the second case it could be a decrease of the binding affinity that occurs concomitantly with the association of the ligand. Because of the displacement, both the radioactivity in the effluent and its depletion from the upper chamber increase.

For the evaluation of the titration curve, it is necessary to compare the instantaneous value of the radioactivity in the effluent with the value that would be found if all L-[^{14}C]-phenylalanine present in the upper chamber were free to diffuse. Since the total radioactivity in this chamber decreases during the titration, the reference values will be on a curve (curve R in Figure 8A). The course of this curve is unknown except that it becomes ultimately identical with that of the observed radioactivity of the effluent when large amounts of unlabeled L-phenylalanine are added. According to what has been said, the reference curve can be constructed, if the decrease of radioactivity in the upper chamber is known during all times of the titration. If the titration curve is divided into segments and if the values of the radioactivity in the center of the segments are, for instance, points 1,..., 7, in Figure 8A, the decrease that corresponds to each of these points can be found as the slopes of the tangents to curve B. This is shown in Figure 8. Curve B has been obtained by a second experiment where the enzyme has been omitted. Curve R is constructed in segments of linear pieces T_1',..., T_7' that have the slopes of the tangents T_1,..., T_7. The pieces are joined together in the way shown in the figure. One starts with T_1' which joins the observed curve for the radioactivity in the effluent after the addition of unlabeled L-phenylalanine. Of course, the resulting curve is only an approximation, which

resembles the theoretical curve R the better the more points on curve A are used (the smaller the segments are). The method is generally applicable.

Acknowledgments

We are deeply indebted to Dr. Mathias Sprinzl, Göttingen, who kindly performed the nucleoside analysis of the HNO_2 deaminated $tRNA^{Phe}$ and provided valuable suggestions.

References

Barrel, B. G., & Sanger, F. (1969) *FEBS Lett. 3*, 275.
Bartmann, P., Hanke, T., Hammer-Raber, B., & Holler, E. (1974) *Biochemistry 13*, 4171.
Bartmann, P., Hanke, T., & Holler, E. (1975a) *J. Biol. Chem. 250*, 7668.
Bartmann, P., Hanke, T., & Holler, E. (1975b) *Biochemistry 14*, 4777.
Blanquet, S., Dessen, P., & Iwatsubo, M. (1976) *J. Mol. Biol. 103*, 765.
Colowick, S. P., & Womack, F. C. (1969) *J. Biol. Chem. 24*, 774.
Eadie, G. S. (1942) *J. Biol. Chem. 146*, 85.
Egan, B. Z., & Kelmers, A D. (1972) *Prep. Biochem., 2*, 265.
Fasiolo, F., Ebel, J.-P., & Lazdunski, M. (1977) *Eur. J. Biochem. 73*, 7.
Favre, A., & Yaniv, M. (1971) *FEBS Lett. 17*, 236.
Fayat, G., Blanquet, S., Dessen, P., Batelier, G., & Waller, J.-P. (1974) *Biochimie 56*, 35.
Fersht, A. R. (1975) *Biocohemistry 14*, 5.
Fersht, A. R., Gangloff, J., & Dirheimer, G. (1978) *Biochemistry 17*, 3740.
Hanke, T., Bartmann, P., Hennecke, H., Kosakowski, H. M., Jaenicke, R., Holler, E., & Böck, A. (1974) *Eur. J. Biochem. 43*, 601.
Holler, E. (1976) *J. Biol. Chem. 251*, 7717.
Holler, E. (1978) *Angew. Chem., Int. Ed. Engl. 17*, 648.
Holler, E., Bennett, E. L., & Calvin, M. (1971) *Biochem. Biophys. Res. Commun. 45*, 409.
Hyafil, F. H., Jacques, Y., Fayat, G., Fromant, M., Dessen, P., & Blanquet, S. (1976) *Biochemistry 15*, 3678.
Jacques, Y., & Blanquet, S. (1977) *Eur. J. Biochem. 79*, 433.
Kosakowski, M. H., & Böck, A. (1970) *Eur. J. Biochem. 12*, 67.
Kosakowski, M. H., & Böck, A. (1971) *Eur. J. Biochem. 24*, 190.
Kosakowski, H. M., & Holler, E. (1973) *Eur. J. Biochem. 38*, 274.
Krauss, G., Pingoud, A., Boehme, D., Riesner, D., Peters, F., & Maass, G. (1975) *Eur. J. Biochem. 55*, 517.
Muench, K. H. (1976) *J. Biol. Chem. 251*, 5195.
Mulvey, R. S., & Fersht, A. R. (1977) *Biochemistry 16*, 4005.
Potts, R., Fournier, M. J., & Ford, N. C. (1977) *Nature (London) 268*, 563.
Roy, K. L., Bloom, A., & Söll, D. (1971) *Prog. Nucleic Acid Res. 2*, 524.
Santi, D. V., & Anderson, R. T. (1974) *Anal. Biochem. 58*, 175.
Scatchard, G. (1949) *Ann. N.Y. Acad. Sci. 51*, 660.
Sprinzl, M., & Faulhammer, H. G. (1979) *Nucleic Acids Res.* (in press).
Uziel, M., & Khym, J. X. (1969) *Biochemistry 8*, 3254.
Yarus, M. (1972) *Proc. Natl. Acad. Sci. U.S.A. 69*, 1915.
Zinoviev, V. V., Rubtsova, N. G., Lavrik, O. I., Malygin, E. G., Akhverdyan, V. Z., Favorova, O. O., & Kisselev, L. L. (1977) *FEBS Lett. 82*, 130.
Zubay, G. (1962) *J. Mol. Biol. 4*, 347.

RNA Replication: Required Intermediates and the Dissociation of Template, Product, and Qβ Replicase†

Carl Dobkin,* Donald R. Mills, Fred Russell Kramer, and Sol Spiegelman

ABSTRACT: Replication complexes containing only one molecule of Qβ replicase and one strand of midivariant RNA (MDV-1 RNA) template were prepared by incubating the replicase with an excess of MDV-1 (−) RNA. In the presence of excess minus strands, these monoenzyme replication complexes were shown to synthesize essentially pure MDV-1 (+) RNA in both the first and second cycles of replication. When an equivalent concentration of mutant MDV-1 (−) RNA was added to this reaction before completion of the first cycle of replication, only wild-type MDV-1 (+) RNA was produced in the first cycle, but both mutant and wild-type MDV-1 (+) RNA were produced in the second cycle of replication. These results demonstrate that a monoenzyme complex is competent to synthesize RNA and, therefore, that a multienzyme replication complex is not a necessary intermediate of replication. The data also imply that after the completion of chain elongation, the product strand is released from the replication complex and that the template and the replicase then dissociate.

This paper concerns several unresolved questions about the mechanism of RNA replication. The interest in RNA replication, catalyzed by the discovery of single-stranded RNA bacterial viruses (Loeb & Zinder, 1961), was dominated by a model derived from the known mechanism of replication of single-stranded DNA bacteriophages. Thus, it was assumed that the first step in RNA replication would be the synthesis of a strand complementary to the viral RNA. This would result in the formation of double-stranded intermediates (designated RF-I), which would then be converted into multistranded intermediates (designated RF-II), consisting of duplexes generating nascent viral "plus" strands. In this model, both RF-I and RF-II are required intermediates, with RF-I

† From the Institute of Cancer Research and the Department of Human Genetics and Development, College of Physicians and Surgeons, Columbia University, New York, New York 10032. *Received November 22, 1978; revised manuscript received February 9, 1979.* This work was supported by National Science Foundation Grant PCM76-22220, American Cancer Society Grant NP-229, National Institutes of Health Grant CA-23767, and U.S. Public Health Service Trainee Grant GM-07419.

0006-2960/79/0418-2038$01.00/0